Neurochemistry International 122 (2019) 73–84

Contents lists available at ScienceDirect

Neurochemistry International

journal homepage: www.elsevier.com/locate/neuint

Autophagy activation alleviates nonylphenol-induced apoptosis in cultured cortical neurons

Siyao Li[a,1], Zhixin Jiang[a,1], Wenjie Chai[a], Yuanyuan Xu[b], Yi Wang[a,*]

[a] Department of Occupational and Environmental Health, School of Public Health, China Medical University, Shenyang, Liaoning, People's Republic of China
[b] Program of Environmental Toxicology, School of Public Health, China Medical University, Shenyang, Liaoning, People's Republic of China

ARTICLE INFO

Keywords:
Nonylphenol
Apoptosis
Autophagy
Primary cortical neurons

ABSTRACT

Emerging evidence indicates that nonylphenol (NP), a widely diffused and stable environmental contaminant, causes damage to the central nervous system (CNS). Although NP could cross the blood-brain barrier (BBB) and accumulate in key brain regions, little is known about the direct effects of NP on neurons. In this study, we aimed to investigate the direct effects of NP exposure on induction of apoptosis and autophagy in primary cortical neurons. Results showed that exposure to NP decreased the cell viability in a concentration-dependent manner. The exposure led to both the increase of TUNEL-positive neurons and the activation of caspase-3. Increased levels of endoplasmic reticulum (ER) stress-related proteins, GRP78, CHOP, ATF4, and casepase-12, were observed in neurons exposed to NP. At the same time, the exposure decreased Bcl-2/Bax ratio and mitochondrial transmembrane potential, and increased the release of Cytochrome-C. In addition, NP exposure enhanced LC3-II conversion, decreased levels of SQSTM1/p62, and increased levels of Beclin-1 and LAMP2. NP exposure also reduced the protein levels of p-mTOR, and did not change the levels of total mTOR. Furthermore, to investigate the role of autophagy in NP-induced apoptosis, both the autophagy inhibitor chloroquine (CQ) and the autophagy inducer rapamycin (RAP) were applied to modulate autophagy activation in primary cortical neurons. The inhibition of autophagy caused by CQ enhanced NP-induced apoptosis; conversely, RAP-induced autophagy remarkably suppressed it. In conclusion, our findings demonstrate that NP exposure induced apoptosis with a concomitant increase of autophagic flux in primary cortical neurons, which supports the idea that this potential neurotoxin has direct effects of on neurons. Both ER stress and mitochondrial pathways may be involved in NP-induced apoptosis in neurons. Furthermore, our results also suggest that autophagy activation might be a protective strategy to ameliorate NP-induced apoptosis in neurons.

1. Introduction

Nonylphenol ethoxylates (NPnEO) are nonionic surfactants widely used in commerce and industry. Nonylphenol (NP) is the main biodegradation of NPnEO and one of the most persistent metabolic products. A broad distribution of NP has been detected in various environmental media including soil, sediment, ground and surface water, food, and bottle water (Careghini et al., 2015). The major route of exposure to NP in humans is food and drink (Arukwe et al., 2000; Careghini et al., 2015). Moreover, it has been found in human samples, such as urine, fetal cord blood, placenta, and breast milk (Huang et al., 2014; Peng et al., 2016). A cohort study of pregnant women in Taiwan demonstrated that urinary NP concentrations was 4.27, 4.21, and 4.10 μg/g cre in the first, second, and third trimesters respectively (Chang et al., 2014). The NP concentration in breast milk collected from Turkish mothers was up to 47.5 ng/ml and the mean NP concentration was 10.1 ng/ml (Sise and Uguz, 2017). A study conducted in pregnant women and their fetuses reported that NP concentrations in fetal cord blood, placenta, and breast milk in the 1st and 3rd months were 18.8 ng/ml, 19.8 ng/g, 23.5 ng/ml, and 57.3 ng/ml, respectively (Huang et al., 2014). Daily NP exposure due to transplacental absorption or via breast milk indicates that fetuses, infants, and children, who are especially vulnerable to negative influences for central nervous system (CNS), are potentially at risk.

Emerging evidence suggests that NP exposure causes damage to CNS, besides its adverse effects on reproductive system, immune system and endocrine system. Mao et al. found maternal exposure to NP resulted in impaired exploration, memory function, and learning ability

* Corresponding author. Department of Occupational and Environmental Health, School of Public Health, China Medical University, No.77 Puhe Road, Shenyang North New Area, Shenyang, Liaoning, 110122, PR China.
E-mail address: wangyi@cmu.edu.cn (Y. Wang).
[1] These authors contributed equally to this work.

https://doi.org/10.1016/j.neuint.2018.11.009
Received 7 August 2018; Received in revised form 12 November 2018; Accepted 13 November 2018
Available online 14 November 2018
0197-0186/

Abbreviations

BBB	blood-brain barrier
BSA	bovine serum albumin
CNS	central nervous system
CQ	chloroquine;
Cyto-C	Cytochrome-C
DAPI	4′,6-diamidino-2-phenylindole
DMEM	Dulbecco's modified Eagle's medium
DMSO	Dimethyl sulfoxide;
ER	Endoplasmic reticulum
FBS	Fetal bovine serum
HBSS	Hank's Balanced Salt Solution
mTOR	the kinase mammalian target of rapamycin
NP	nonylphenol
NPnEO	Nonylphenol ethoxylates
PBS	phosphate buffered saline;
p-mTOR	phosphorylated mTOR
TBST	Tris-buffered saline with Tween 20
TUNEL	terminal deoxynucleotidyl transferase dUTP nick end labelling
RAP	rapamycin

in offspring mice (Mao et al., 2010). Rats orally administrated NP for 35 days showed poor performance in elevated plus maze and Morris water maze test (Kazemi et al., 2018). Another study showed that exposure to NP resulted in neurochemical and histopathological perturbations in frontal cortex and hippocampus, in addition to cognitive functions (Tabassum et al., 2017). F1 male rats exposed to NP from gestational day 9–15 demonstrated impaired escape behaviors and learning and memory functions (Jie et al., 2010). The above studies indicate that NP is a potential toxicant that induces neurotoxicity *in vivo* conditions, although the mechanism remains unclear. As an environmental endocrine disruptor, NP may interfere with the body's endocrine systems, which may contribute to its damage to CNS. However, it should be noted that NP could cross the blood-brain barrier (BBB) and accumulate in some key brain regions for learning and memory (Kazemi et al., 2018). Thus, it is interesting and worthwhile to investigate the direct effects of this potential neurotoxin on neurons.

Autophagy is a self-degradative process where lysosomal degradation eradicates the damaged cellular components and misfolded proteins, to play house-keeping roles (Mizushima and Komatsu, 2011). It participates in many aspects of growth, development, metabolism, proliferation, differentiation, and aging of cells (Yang and Klionsky, 2010). Autophagy can be activated by a variety of intracellular or extracellular signals. Although some mechanisms underlying autophagy remain to be elucidated, the kinase mammalian target of rapamycin (mTOR) and Beclin-1 are believed to play crucial roles in the regulation of autophagy (Kang et al., 2011; Ryter et al., 2014; Yu et al., 2017). Under certain conditions, autophagy involves in the stress adaptation that avoids cell death, but in other situations, the autophagic process could lead to cell death (Xi et al., 2013).

Apoptosis, as well as autophagy, is a basic biological process and essential for maintaining homeostasis. However, abnormal apoptosis can be triggered by various stress stimuli. As previously reported, NP exposure activated caspase-3, a hallmark of apoptosis, in mouse hippocampal cells *in vitro* (Litwa et al., 2016), and induced apoptosis in mouse brain *in vivo* (Mao et al., 2008), although the mechanism underlying NP-induced apoptosis still remains to be elucidated. Mitochondrial and endoplasmic reticulum (ER) stress pathways are two critical intrinsic pathways of apoptotic cell death (Malhotra and Kaufman, 2011; Wang et al., 2011). ER stress is intimately connected with the mitochondrial pathway in apoptotic signaling (Malhotra and Kaufman, 2011; Wang et al., 2011). ER stress could alter the expression of Bcl-2 family members, lead to mitochondrial dysfunction (Nutt et al., 2002; Tabas and Ron, 2011), cause Cytochrome-C (Cyto-C) release from mitochondria, trigger the activation of terminal caspases, and thereby induce apoptotic cell death (Cao et al., 2001; Green and Reed, 1998).

Both autophagy and apoptosis may cause programmed cell death and regulate cell survival (Song et al., 2017). The relationship between autophagy and apoptosis is very complicated and greatly affects cellar homeostasis (Kesidou et al., 2013; Xi et al., 2013). It has been shown that in some cases, autophagic process, induced by diverse stress stimuli, ultimately leads to apoptotic cell death; however, in other instances, it prevents the apoptotic process (Zhang et al., 2017). In addition, sometimes autophagy and apoptosis seem to be two comparatively independent processes (Mizushima and Komatsu, 2011). Although NP-induced apoptosis in neurons has been observed in previous studies (Litwa et al., 2016; Mao et al., 2008), the effect of NP on autophagy in neurons has not been investigated, not to mention the cross-talk between them.

Hence, this study aimed to explore the direct effects of NP exposure on apoptosis in primary cortical neurons, and for the first time, examine whether NP exposure caused autophagy in neurons. The critical pathways of apoptosis, ER stress and mitochondrial pathways, were also investigated to further study the NP-induced apoptosis. Furthermore, by administrating of chloroquine (CQ) or rapamycin (RAP) as a tool to modulate autophagy activation, we illuminated the role of autophagy in apoptosis of cortical neurons induced by NP. The unraveling this role may provide new clues to elucidate the mechanisms underlying the NP-induced neurotoxicity.

2. Materials and methods

2.1. Reagents

4-n-Nonylphenol (NP, ≥99.0%) was purchased from Dr. Ehrenstorfer (Augsburg, Germany). CellTiter 96® AQueous One Solution Cell Proliferation Assay (MTS) and DeadEnd™ Fluorometric TUNEL System were from Promega (Madison, WI, USA). Neurobasal-A Medium, B27 supplement, Penicillin-Streptomycin, Trypsin-EDTA, Dulbecco's modified Eagle's medium (DMEM), and Hank's Balanced Salt Solution (HBSS) were from GIBCO/Invitrogen (Carlsbad, CA, USA). Fetal bovine serum (FBS) was from Hyclone (Legan, UT, USA). β-D-arabinofuranoside, Poly-L-lysine, Glutamine, CQ, RAP, and Dimethyl sulfoxide (DMSO) were from Sigma-Aldrich (St. Louis, MO, USA). Pierce BCA protein assay reagent and DAPI (4′,6-diamidino-2-phenylindole) were from Thermo Scientific (Rockford, IL, USA). Mitochondrial membrane potential assay kit was from Beyotime (Shanghai, China). Primary antibodies of MAP2, Cyto-C, and β-actin were obtained from Santa Cruz Biotechnology (Santa Cruz, CA, USA). Primary antibodies of cleaved caspase-3, mTOR and phosphorylated (p)-mTOR, LC3-I/II, Bax, COX IV, and Beclin-1 were from Cell Signaling Technology (Beverly, MA, USA). Primary antibodies of LAMP2, SQSTM1/p62, Bcl-2 and NeuN were obtained from Abcam (Cambridge, MA, USA). Primary antibodies of ATF4, Caspase-12, CHOP, and GRP78 were obtained from Proteintech (Rosemont, IL, USA).

2.2. Cortical neurons culture

Healthy Wistar rats were obtained from the Center for Experimental Animals at China Medical University (Shenyang, China). The experimental protocol was approved by the Animal Use and Care Committee, China Medical University, which complies with the National Institutes of Health Guide for the Care and Use of Laboratory Animals (NIH Publications No. 8023, revised 1978). Rats were housed at temperature 24 ± 1 °C with a 12/12-h light and dark cycle. Standard rat pellet diet

and potable water were provided *ad libitum*. After acclimation for 1 week, female rats were mated with male rats (♀:♂ = 2:1). All efforts were made to minimize animal suffering, to reduce the number of animals used, and to utilize alternatives to *in vivo* techniques, if available.

Primary cortical neurons were prepared from brains of newborn pups on postnatal day 1. Briefly, newborn pups were immersed in 75% ethanol for about 20 s, then the pups were rapidly decapitated to remove their cortices. Cortices were washed in cold D-Hanks before being dissected into small pieces, and incubated in 0.125% trypsin at 37 °C for 20 min. The digestion was terminated by adding 20% fetal bovine serum (FBS). The cell suspension was filtered from the tissue by using a cell strainer (200 μm). The suspension was centrifuged at 1200 r/min for 5 min and cells were acquired by removing the supernatant liquid. The cells were re-suspended in DMEM medium containing 10% FBS. The re-suspended cell suspension was filtered again by using a cell strainer (70 μm) and the cell density of 10^6 cell/ml was adjusted before being seeded onto pre-coated poly-L-lysine plastic culture plates. After 24 h, the DMEM medium was replaced by Neurobasal medium supplemented with B27, penicillin-streptomycin, and glutamine. After 48 h, Cytosine β-D-arabinofuranoside (3.33 μM) was added into the medium in order to inhibit glia proliferation. From then on, half of the culture medium was replaced by fresh Neurobasal medium every other day. 7 days later, the follow-up experiments were performed.

To assess the purity of cultured neurons, MAP2 (neuron marker) and DAPI (cell nucleus marker) were analyzed by immunofluorescence (Supplementary Fig. 1) in cultured cells. 100 cells were randomly selected and the number of MAP2 positive cells was counted. The percentage of MAP2 positive cells was above 90% in this study.

On day *in vitro* 7, neurons were treated with indicated concentration of NP for 24 h. To further explore the role of autophagy in NP-induced apoptosis, primary cultured cortical neurons were treated with NP (50 μM) in the presence of CQ (30 nM) or RAP (300 nM) for 24 h.

2.3. MTS assay

Neurons were cultured in a poly-L-lysine-coated 96-well culture plate (5×10^4 cells per well). On day *in vitro* 7, neurons were treated with 100 μl of the growth medium in the presence or absence of NP, CQ, or RAP. Then neurons were cultured at 37 °C in 5% CO_2 for 22 h. At the end of treatment, 20 μl of MTS solution was added to each well, and the plates were incubated at 37 °C for additional 2 h. Then, the absorbance values of each well were measured at 490 nm using a microplate reader (Multiscan Ascent, Labsystem, Finland). The results were expressed as percentage of control value.

2.4. TUNEL assay

Apoptosis was monitored by the TUNEL (terminal deoxynucleotidyl transferase dUTP nick end labelling) staining using a DeadEnd™ Fluorometric TUNEL System according to the manufacturer's instructions (Promega, USA). Briefly, neurons were cultured in a poly-L-lysine-coated 12-well plates. On day *in vitro* 7, neurons were treated with NP in the presence or absence of CQ or RAP. At the end of the treatment, neurons were washed with phosphate buffered saline (PBS) twice, and then fixed with 4% paraformaldehyde solution for 30 min at 4 °C and permeabilized with Triton® X-100 at room temperature for 15 min. After being equilibrated at room temperature for 5–10 min, neurons were labeled DNA strand breaks with fluorescein-12-dUTP at 37 °C for 60 min. Finally, the reaction was terminated with 2 × SSC. Localized green fluorescence of apoptotic cells (fluorescein-12-dUTP) was detected by fluorescence microscopy (DMIRB Microscope, Leica).

2.5. Western blotting analysis

Neurons were cultured in poly-L-lysine-coated 6-well plates and prepared for protein extracts. At the end of treatment mentioned above, neurons were washed with ice-cold PBS, scraped by “policeman”, and harvested in RIPA Lysis Buffer supplemented with protease inhibitors and phosphatase inhibitors at 4 °C for 30 min. Lysates were cleared by centrifugation at 12000 r/min at 4 °C for 5 min. Then, supernatants were collected. The mitochondria/cytosol fractionation kit was purchased from Wanlei Biotech (Shenyang, China). The isolation of mitochondria/cytosol protein was performed according to the manufacturer's instruction. Protein concentrations were determined using Pierce BCA protein assay reagent. Protein extracts were analyzed by Western blotting according to the standard protocols. In brief, protein extracts were loaded and separated by sodium dodecyl sulfate-polyacrylamide gel electrophoresis (SDS-PAGE). Subsequently, the proteins were transferred to a PVDF membrane (Millipore, USA). After blocking in 5% bovine serum albumin (BSA) for 1 h, the membranes were incubated with primary antibodies (anti-LC3-I/II; anti-SQSTM1/p62; anti-cleaved caspase-3; anti-LAMP2; anti-Beclin-1; anti-mTOR; anti-p-mTOR; anti-ATF4; anti-caspase-12; anti-Bcl-2; anti-Bax; anti-CHOP; anti-GRP78; anti-Cyto-C; anti-COX IV; anti-β-actin) overnight (4 °C) at 1:800-5000 dilutions. After washing with Tween 20/Tris-buffered saline (TBST), membranes were incubated with secondary antibody (Santa Cruz Biotechnology, CA, USA) for 1 h at 37 °C. The membranes were detected by chemiluminescence system (Thermo Scientific). The quantitative analysis was carried out by NIH ImageJ program and normalized to β-actin or COX IV (loading control for mitochondrial protein) in each sample.

2.6. Immunofluorescence analysis

Neurons were cultured on poly-L-lysine-coated glass coverslips and prepared for immunofluorescence. At the end of treatment mentioned above, neurons were washed with PBS twice, fixed with 4% paraformaldehyde solution for 30 min at 4 °C, and permeabilized with Triton X-100 at room temperature for 15 min. After blocking with 5% goat serum albumin for 1 h, neurons were incubated with primary antibodies (anti-LC3-I/II; anti-SQSTM1/p62; anti-NeuN; anti-MAP2) overnight (4 °C) at 1:200-1000 dilutions. After washing with PBS, neurons were incubated with secondary antibodies for 1 h at room temperature. The glass coverslips were rinsed in PBS, taken out from 24-well plates, and gently placed (neurons facing down) on the glass slide. The samples were analyzed with a fluorescence confocal microscopy (A1R, Nikon).

2.7. Mitochondrial membrane potential analysis

JC-1 mitochondrial membrane potential assay kit was used to monitor the mitochondrial transmembrane potential. In healthy neurons with physiological mitochondrial transmembrane potential, JC-1 dye enters into the mitochondrial matrix and forms J-aggregates with red fluorescence. However, JC-1 dye remains in the monomeric form with green fluorescence in the cytoplasm, when the mitochondrial membrane potential is depolarized (Perry et al., 2011). The experiment was conducted according to the manufacturer's instruction. Briefly, neurons were cultured in poly-L-lysine-coated 24-well plates. After the treatments, neurons were washed with PBS and incubated with JC-1 in the dark for 20 min at 37 °C. Then, neurons were washed with staining buffer twice. Images were captured under fluorescence microscope (RVL-100, Echo laboratories) and analyzed by NIH ImageJ program.

2.8. Statistics

All experiments were performed in at least triplicate. Data are shown as mean ± standard deviation (SD). Statistical analyses were performed using SPSS 16.0 software. Statistical significance was assessed by one-way analysis of variance followed by Student-Newman-Keuls test. $p < 0.05$ was considered statistically significant.

3. Results

3.1. NP decreased neuronal cell viability in a dose-dependent manner

In order to study the cytotoxicity of NP in neurons, primary cortical neurons were treated with different concentrations of NP and cell viability was measured by the MTS assay. The neurons treated with NP showed a dose dependent decrease in the cell viability compared to vehicle controls (Fig. 1). Treatment with 0.01, 0.1 and 1 μM NP did not significantly reduced the cell viability. However, at higher concentrations from 10 to 100 μM, NP showed significantly cytotoxic effect on neurons ($p < 0.05$). 30, 50, and 70 μM NP, in which the survival rate was above 80%, were used to conduct further experiments.

3.2. NP induced apoptosis in primary cortical neurons

To determine whether NP could induce apoptosis in cortical neurons, the TUNEL (terminal deoxynucleotidyl transferase-mediated dUTP nick-end labelling) assay was performed. The TUNEL assay detects DNA fragmentation, which is the characteristic of apoptotic cell death (Shen et al., 2000). TUNEL-positive cells were occasionally found in the control group, but apoptotic neurons were increased by incremental doses of NP (Fig. 2A). Treatment with NP at 30, 50, and 70 μM significantly increased TUNEL-positive cells to 1.5-fold, 1.9-fold, and 2.6-fold of the control values, respectively ($p < 0.05$). To further confirm the apoptosis induced by NP treatment, cleaved-caspase-3 protein expression, which is also used as a hallmark of apoptosis, was detected by Western blotting analysis. Similar to the results of TUNEL assay, NP caused an obviously dose-dependent increase in cleaved caspase-3 protein levels (Fig. 2B). The cleaved caspase-3 protein levels were increased from 149% to 205% of the control value as NP concentration increased from 30 to 70 μM, although the difference was not significant between the control and 30 μM treatment groups.

3.3. NP induced ER stress in primary cortical neurons

To determine whether ER stress was involved in NP-induced apoptosis, we studied ER stress-related proteins or markers, such as GRP78, ATF4, CHOP, and casepase-12, in primary cortical neurons by Western blotting analysis. Treatment with NP at 50 and 70 μM significantly increased the expression of GRP78 in neurons to 1.8-fold and 2.0-fold of the control value, respectively ($p < 0.05$, Fig. 2C). Treatment with NP at 30 μM tended to increase the expression of GRP78, although the increase was not significant. As for ATF4 expression, a significant increase in dose-dependent manner was observed upon exposure to 30, 50, and 70 μM NP (1.3-fold, 1.4-fold, and 1.5-fold of the control value, respectively; $p < 0.05$, Fig. 2D). Treatment with NP at 70 μM significantly increased the expression of CHOP in neurons to 1.4-fold of the control value ($p < 0.05$, Fig. 2E). As a pivotal factor in the ER stress pathway, casepase-12 is specifically activated by ER stress (Nakagawa et al., 2000). Treatment with NP at 50 and 70 μM significantly increased the expression of cleaved casepase-12 in neurons to 1.53-fold and 1.54-fold of the control value, respectively ($p < 0.05$, Fig. 2F). Treatment with NP at 30 μM tended to increase the expression of cleaved casepase-12, but the increase was not significant.

3.4. NP altered mitochondria-dependent pathway of apoptosis in primary cortical neurons

To investigate the involvement of mitochondrial dysregulation in NP-induced apoptosis of primary cortical neurons, the ratio of Bcl-2/Bax, the mitochondrial membrane potential, and the release of Cyto-C were detected. Treatment with NP at 50 and 70 μM significantly increased the expression of pro-apoptotic Bax and significantly decreased the expression of anti-apoptotic Bcl-2 ($p < 0.05$, Fig. 3A). Furthermore, significant decrease of Bcl-2/Bax ratio was found in all NP treatment groups ($p < 0.05$, Fig. 3A). The alteration of mitochondrial membrane potential was detected by JC-1 fluorescence assay. Our result showed that NP treatment led to an increase in green fluorescence and a decrease in red fluorescence (Fig. 3B). Further analysis revealed that treatment with NP at 30, 50, and 70 μM significantly decreased the red: green fluorescent ratio to 65, 38, and 6% of control value ($p < 0.05$, Fig. 3C). These data indicated NP treatment caused an obvious reduction in the mitochondrial membrane potential in neurons. We also investigated the effect of NP exposure on the release of Cyto-C from the mitochondria by Western blotting. Treatment with NP at 50 and 70 μM was found to significantly increase Cyto-C levels in the cytosol to 1.5-fold and 2.1-fold of the control value, respectively ($p < 0.05$, Fig. 3D), while significantly decrease Cyto-C levels in the mitochondria ($p < 0.05$, Fig. 3E). Cyto-C levels tended to increase in the cytosol and decrease in the mitochondria in response to 30 μM of NP, though the differences were not significant.

3.5. NP Activated Autophagy in primary cortical neurons

We investigated the effect of NP treatment on autophagy activity in cultured cortical neurons. The autophagic specific protein LC3 was examined in this study. LC3 protein in the cytoplasm is converted from LC3-I into LC3-II, when the autophagy is activated. Thus, the ratio of the LC3-II/LC3-I and the amount of the LC3-II protein are often used to assess the activation of autophagy (Zhou et al., 2017b). We found that treatment with NP at 50 and 70 μM NP significantly increased the ratio of the LC3-II/LC3-I to 1.4-fold, and 1.6-fold of the control value, respectively ($p < 0.05$, Fig. 4A). In addition, a 1.2-fold increase in the ratio of the LC3-II/LC3-I was observed in 30 μM NP treatment neurons, although it was not significant. The results of immunofluorescence also showed that NP treatment increased the expression of LC3-II in neurons compared with the control (Fig. 4B).

Increased autophagic activity results in the depletion of SQSTM1/p62, a well-known autophagic substrate (Sarkar et al., 2014). Treatment with 30, 50 and 70 μM NP significantly reduced the levels of SQSTM1/p62 in neurons to 75, 57, and 45% of the control value, respectively ($p < 0.05$, Fig. 4C). Immunofluorescence analysis also confirmed that NP treatment reduced the expression of SQSTM1/p62 in neurons (Fig. 4D).

As an important membrane protein of lysosomes, lysosomal-associated membrane protein 2 (LAMP2) is required for autophagosome-lysosome fusion and degradation, and thereby contributes to autophagic flux (Zhou et al., 2018). Treatment with NP at 70 μM significantly

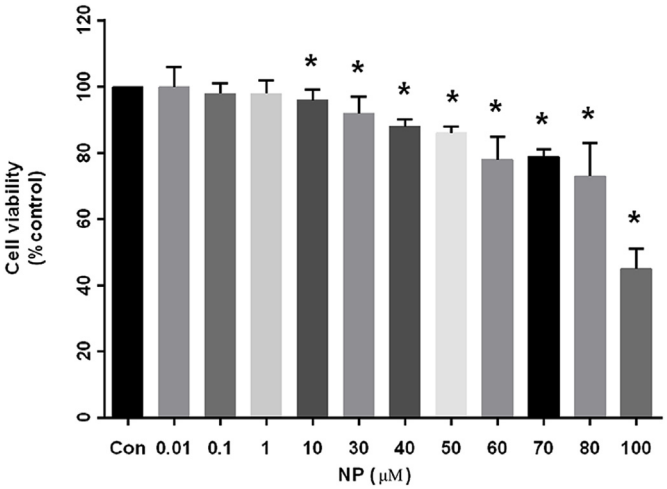

Fig. 1. NP decreased neuronal cell viability in a dose-dependent manner. MTS assay was used to assess neuronal cell viability following the treatment of NP (0.01–100 μM) for 24 h. The values are expressed as mean ± SD (n = 6). *$p < 0.05$ vs. control group.

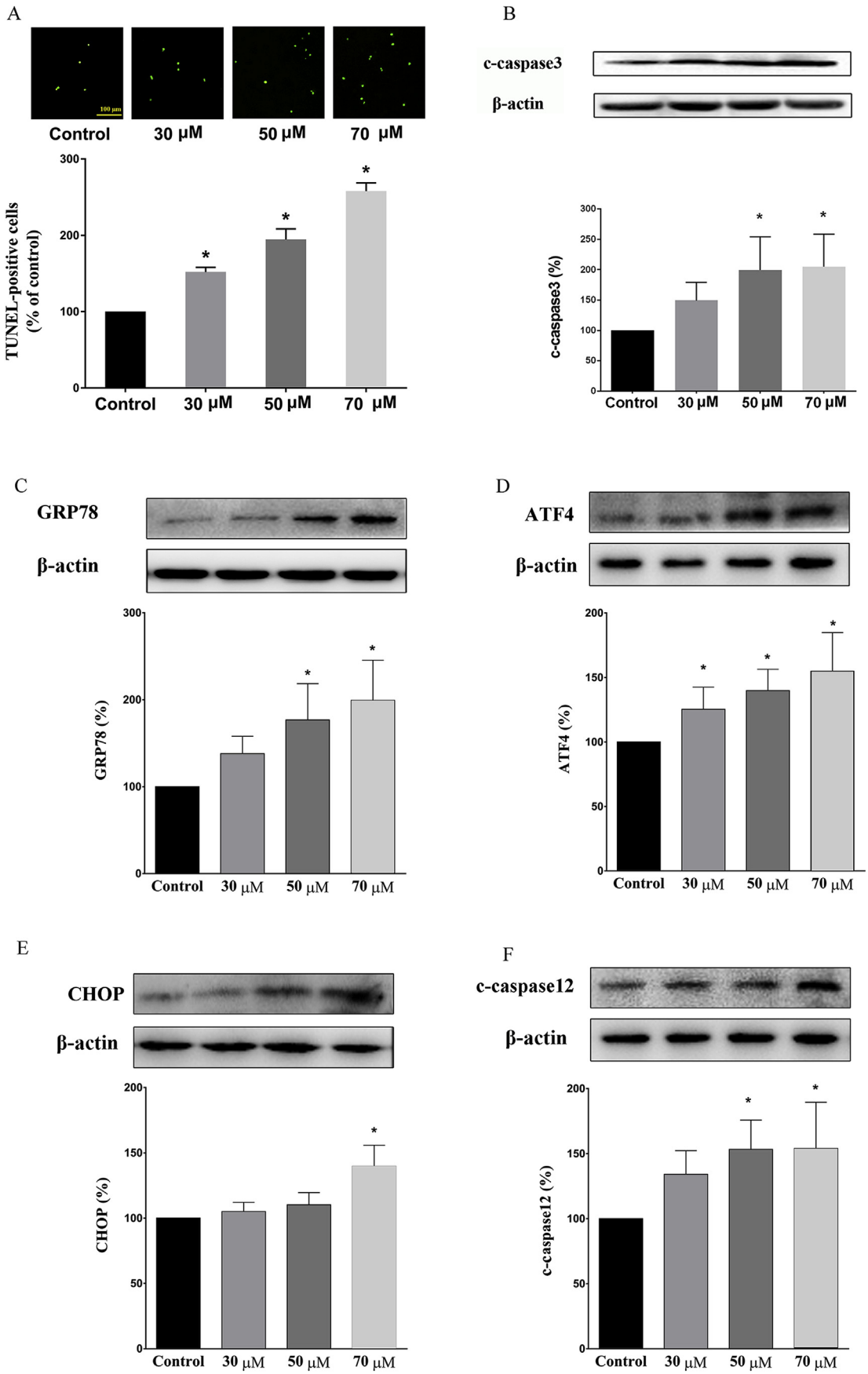

Fig. 2. NP induced apoptosis and ER stress in cortical neurons. (A) Representative images of TUNEL-positive neurons from all treatment groups. Green fluorescence indicates the apoptotic cells. Quantitative analysis of TUNEL-positive cells is shown in the lower bar graphs. (B), (C), (D), (E), (F) Western blotting for the expression of c-caspase3, GRP78, ATF4, CHOP, c-caspase12. The upper bands depict representative findings for neurons from all treatment groups. The lower bar graphs show the results of the semi-quantitative measurement of the protein. Each bar represents the mean ± SD (n = 4). *p < 0.05 vs. control group.

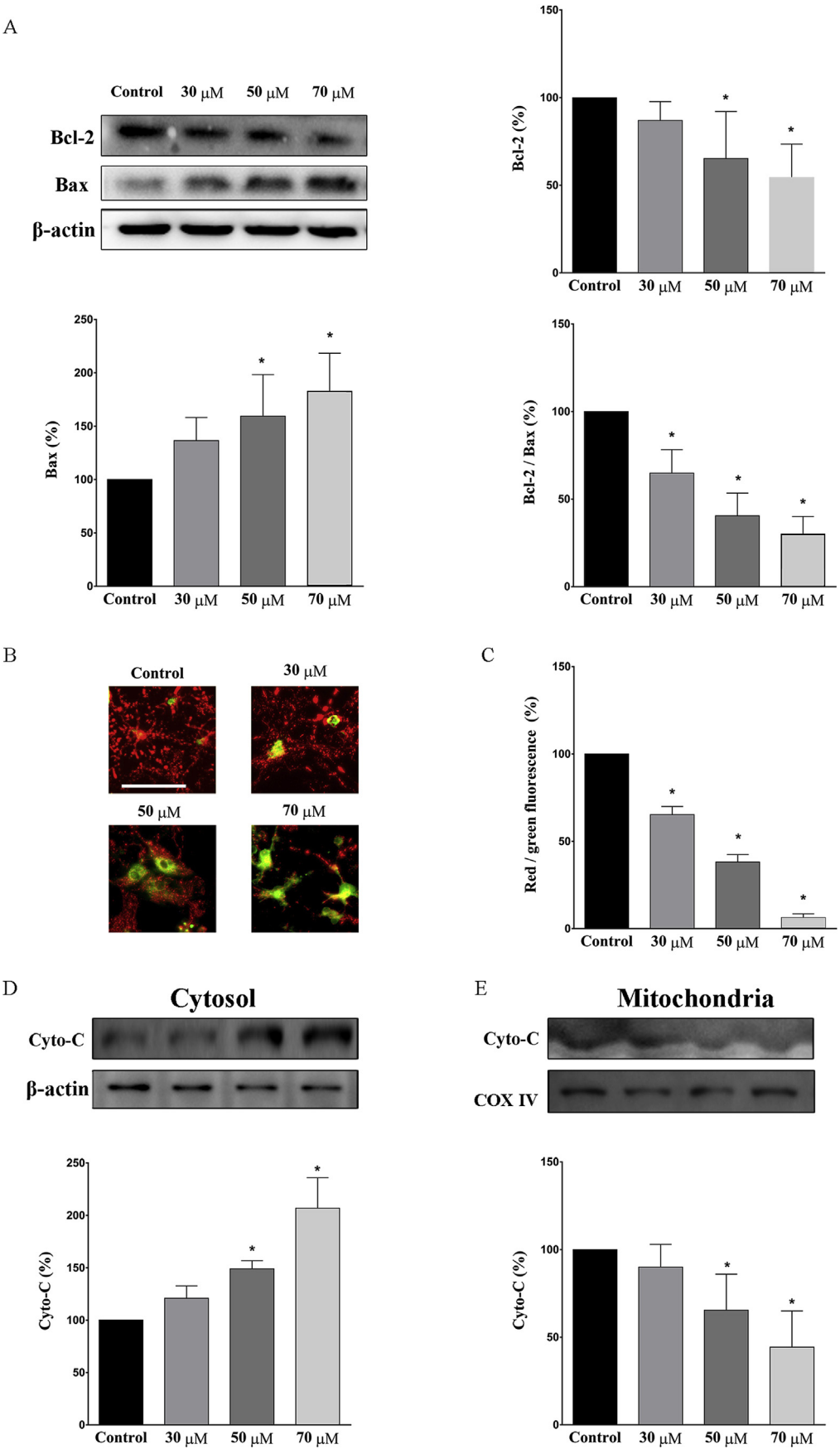

Fig. 3. NP altered mitochondria-dependent pathway of apoptosis in primary cortical neurons. (A) Western blotting for the expression of Bcl-2 and Bax. The upper bands depict representative findings for neurons from all treatment groups. The lower bar graphs show the results of the semi-quantitative measurement of the Bax, Bcl-2, and the ratio of Bcl-2 to Bax. Each bar represents the mean ± SD (n = 4). *p < 0.05 vs. control group. (B) Representative images of neurons stained by JC-1. A shift from red (JC-1 aggregates, high mitochondrial membrane potential) to green (JC-1 monomers, low mitochondrial membrane potential) fluorescence was induced by NP exposure in neurons. Scale bar = 50 μm. (C) Quantitative analysis of red: green fluorescent ratio is shown in the bar graphs. Each bar represents the mean ± SD (n = 6). *p < 0.05 vs. control group. (D), (E) Western blotting for the level of Cyto-C in the cytosol and mitochondria. The upper bands depict representative findings for neurons from all treatment groups. The lower bar graphs show the results of the semi-quantitative measurement of the corresponding protein. Each bar represents the mean ± SD (n = 4). *p < 0.05 vs. control group.

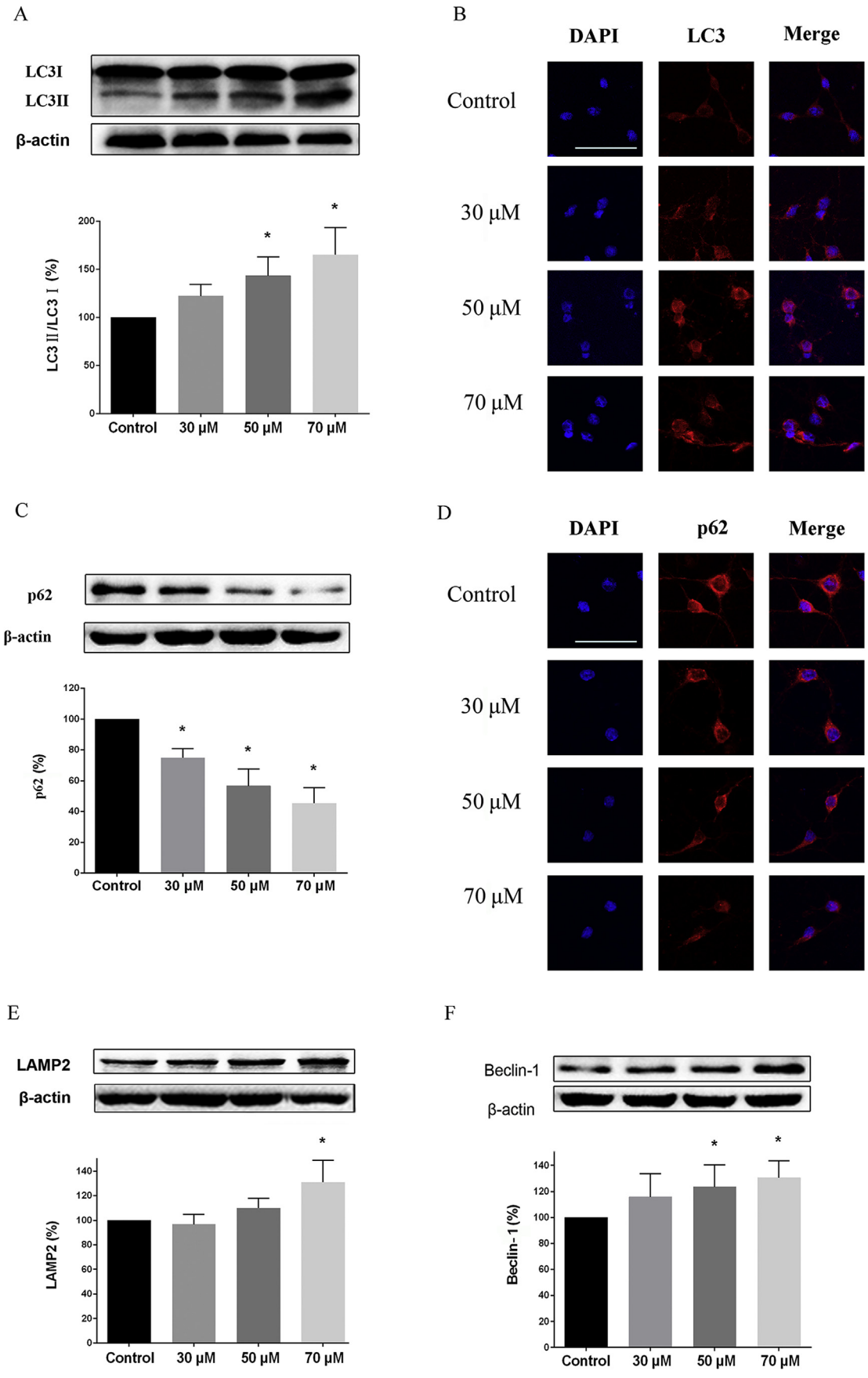

(caption on next page)

Fig. 4. NP Activated Autophagy in cortical neurons. (A), (C), (E), (F) Western blotting for the expression of LC3-II/LC3-I, SQSTM1/p62, LAMP2 and Beclin-1. The upper bands depict representative findings for neurons from all treatment groups. The lower bar graphs show the results of the semi-quantitative measurement of the corresponding protein. Each bar represents the mean ± SD (n = 4). *p < 0.05 vs. control group. (B) Representative images of neurons stained with anti-LC3-II (red) and DAPI (blue). (D) Representative images of neurons stained with anti-SQSTM1/p62 and DAPI (blue). The images were obtained under the same conditions at a magnification of 400 × across groups. Scale bar = 50 μm.

increased the expression of LAMP2 in neurons to 1.3-fold of the control value ($p < 0.05$, Fig. 4E). Treatment with NP at 50 μM tended to increase the expression of LAMP2, but the increase was not significant.

Beclin-1 is an important autophagy-related protein, which is required for the formation of preautophagosomal structures (Li et al., 2014). Treatment with NP at 50 and 70 μM significantly increased the expression of Beclin-1 in neurons to 1.2-fold and 1.3-fold of the control value, respectively ($p < 0.05$, Fig. 4F). Treatment with NP at 30 μM tended to increase the expression of Beclin-1, although the increase was not significant.

3.6. NP decreased phosphorylation of mTOR in primary cortical neurons

Mammalian target of rapamycin (mTOR) plays a central role in regulating of autophagy induction. Its activation is believed to negatively regulate autophagy (Singh et al., 2017). The phosphorylation of mTOR at Ser 2448 was detected to assess its activation. Exposure to NP (30, 50, and 70 μM) significantly decreased p-mTOR levels to 73, 63, and 52% of the control values, respectively ($p < 0.05$, Fig. 5A). However, treatment with NP at various concentrations did not affect levels of total mTOR (Fig. 5B).

3.7. Inhibition of autophagy promoted NP-induced apoptosis in primary cortical neurons

CQ is widely used as a pharmacological inhibitor of autophagic pathway (Yoon et al., 2010). To further clarify the role of autophagy in NP-induced apoptosis in neurons, CQ was employed in this study. The MTS assay showed that treatment of neurons with NP and CQ significantly reduced the cell viability than treatment with NP alone (0.88-fold of the value in 50 μM NP-treated neurons, $p < 0.05$, Fig. 6A). The TUNEL assay showed that treatment of neurons with NP and CQ significantly increased the number of TUNEL-positive cells than treatment with NP alone (1.4-fold of the value in 50 μM NP-treated neurons, $p < 0.05$, Fig. 6B).

In addition, similar to the results of TUNEL assay, treatment of neurons with NP and CQ caused a significant increase in cleaved caspase-3 protein level than treatment with NP alone (1.5-fold of the value in 50 μM NP-treated neurons, $p < 0.05$, Fig. 6C). Taken together, these results indicated that inhibition of autophagy promoted NP-induced apoptosis in cortical neurons. Additionally, to confirm the inhibition of autophagic flux induced by CQ, autophagic substrate SQSTM1/p62 was detected in neurons. In line with expectations, CQ significantly increased SQSTM1/p62 levels when compared with NP treated alone ($p < 0.05$, Supplementary Fig. 2).

3.8. Activation of autophagy reduced NP-induced apoptosis in primary cortical neurons

RAP, an antibiotic derived from Streptomyces hygroscopius, is commonly used to activate autophagy (Singh et al., 2017). To further explore the relationship between autophagy and apoptosis caused by NP in neurons, we examined the effect of RAP on NP-induced apoptosis in neurons. The MTS assay showed that treatment of neurons with NP and RAP significantly increased the cell viability than treatment with NP alone (1.1-fold of the value in 50 μM NP-treated neurons, $p < 0.05$, Fig. 7A). The TUNEL assay indicated that treatment of neurons with NP and RAP significantly reduced the number of apoptotic neurons than treatment with NP alone (65% of the value in 50 μM NP-treated neurons, $p < 0.05$, Fig. 7B). Consistent with the results of TUNEL assay, treatment of neurons with NP and RAP caused a significant decrease in cleaved caspase-3 protein level than treatment with NP alone (67% of the value in 50 μM NP-treated neurons, $p < 0.05$, Fig. 7C). In addition, RAP significantly decreased autophagic substrate SQSTM1/p62 levels in neurons when compared with NP treated alone ($p < 0.05$, Supplementary Fig. 3), which confirmed activation of autophagy induced by RAP.

4. Discussion

Increasing evidence indicates that NP is a neurotoxin that causes cognitive and behavioral alterations. Notably, previous studies have

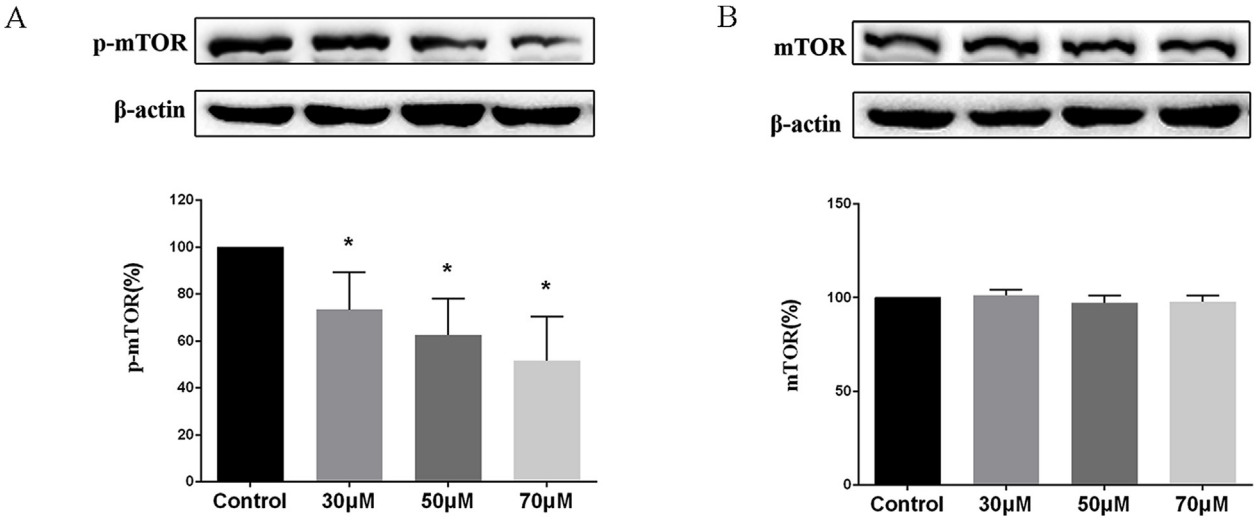

Fig. 5. NP decreased phosphorylation of mTOR in cortical neurons. (A), (B) Western blotting for the expression of p-mTOR and mTOR. The upper bands depict representative findings for neurons from all treatment groups. The lower bar graphs show the results of the semi-quantitative measurement of the corresponding protein. Each bar represents the mean ± SD (n = 4). *p < 0.05 vs. control group.

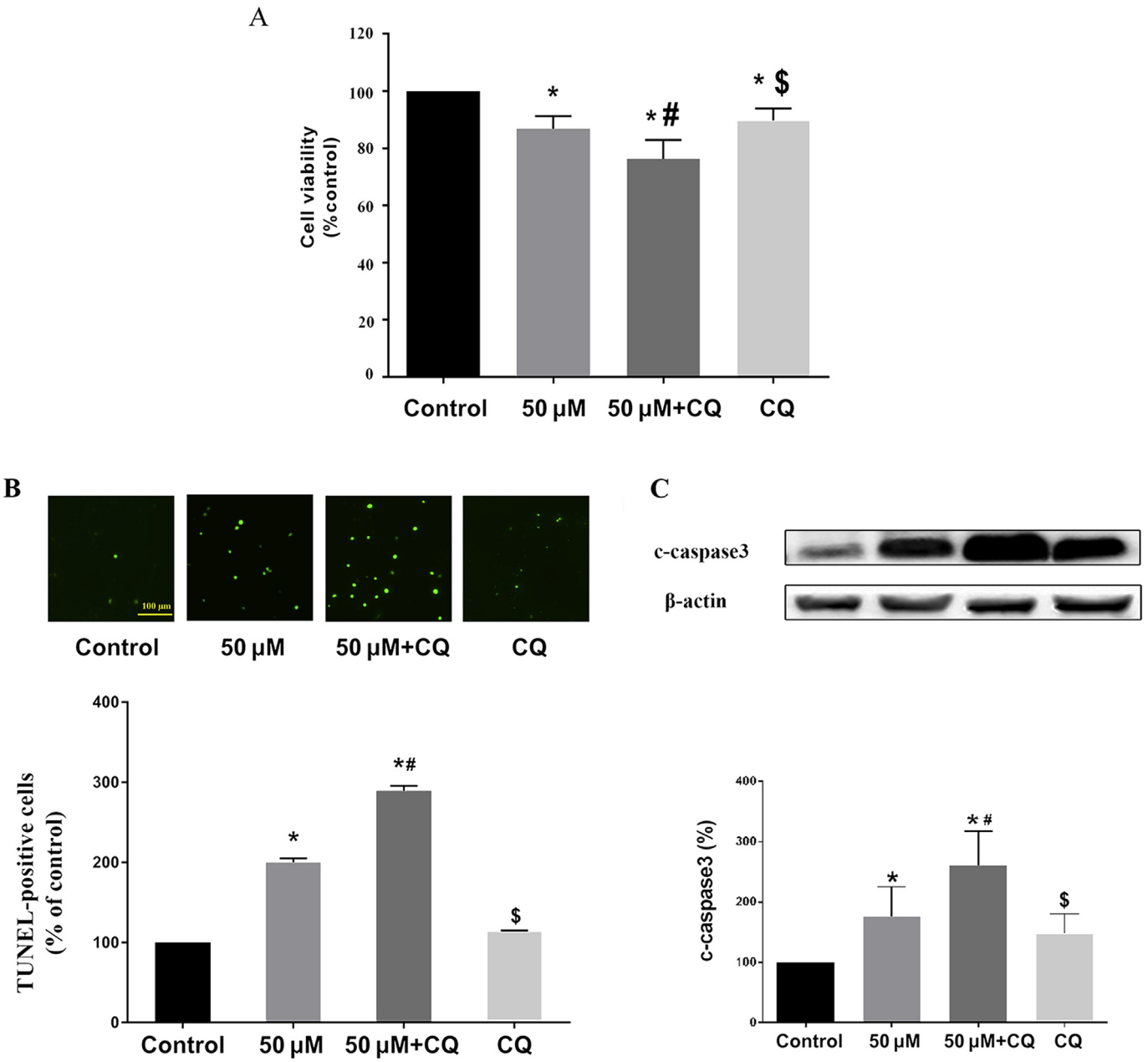

Fig. 6. Inhibition of autophagy promoted NP-induced apoptosis in cortical neurons. Cultured cortical neurons were treated with 50 μM NP and with/without 30 nM CQ for 24 h (A) MTS assay was used to assess neuronal cell viability in all treatment groups. The values are expressed as mean ± SD (n = 4). (B) Representative images of TUNEL-positive neurons from all treatment groups. Green fluorescence indicates the apoptotic cells. Quantitative analysis of TUNEL-positive cells is shown in the lower bar graphs. (C) Western blotting for the expression of apoptotic marker c-caspase3 in neurons. The upper bands depict representative findings for neurons from all treatment groups. The lower bar graphs show the results of the semi-quantitative measurement of the protein. Each bar represents the mean ± SD (n = 4). *p < 0.05 vs. control group; $^{\#}$p < 0.05. vs. 50 μM group; $^{\$}$ p < 0.05. vs. 50 μM + CQ group.

found that its neurotoxic effects are related to the abnormal induction of apoptosis in nerve cells (Litwa et al., 2014; Mao et al., 2008). NP is a well-known endocrine disruptor. Therefore, the disturbance of endocrine systems caused by NP may involve in the abnormal induction of apoptosis in neurons *in vivo*. However, its direct effect on the induction of apoptosis in neurons cannot be ruled out, and especially it could cross the BBB (Kazemi et al., 2018). Thus, the direct effects of NP on apoptosis using primary cortical neurons were investigated in this study.

In addition to apoptosis, we investigated the direct effects of NP on cell viability. Treatment with 0.01–100 μM NP led to a dose-dependent decrease of cell viability in primary cortical neurons. In addition, cell viability was greatly reduced in neurons treated with 10 μM NP or more. These results indicated exposure to NP directly induced cytotoxicity in cultured cortical neurons. Several previous studies also reported that NP induced cytotoxicity in other neuronal cell types. In neural stem cells, NP significantly decreased viability at concentrations over 3 μM (Kudo et al., 2004). Meanwhile, NP significantly decreased the viability of PC12 cells over 56 μM (Kusunoki et al., 2008). The difference of NP concentrations to induce cytotoxicity may be attributed to different experimental designs and neurocyte types.

NP has been shown to induce apoptosis in the gastrointestinal or reproductive cells (Lepretti et al., 2015; Tang et al., 2017). It also triggered apoptosis of murine hippocampal cells and neural stem cells (Kudo et al., 2004; Litwa et al., 2016). In this study, we found that NP exposure increased TUNEL-positive primary cortical neurons.

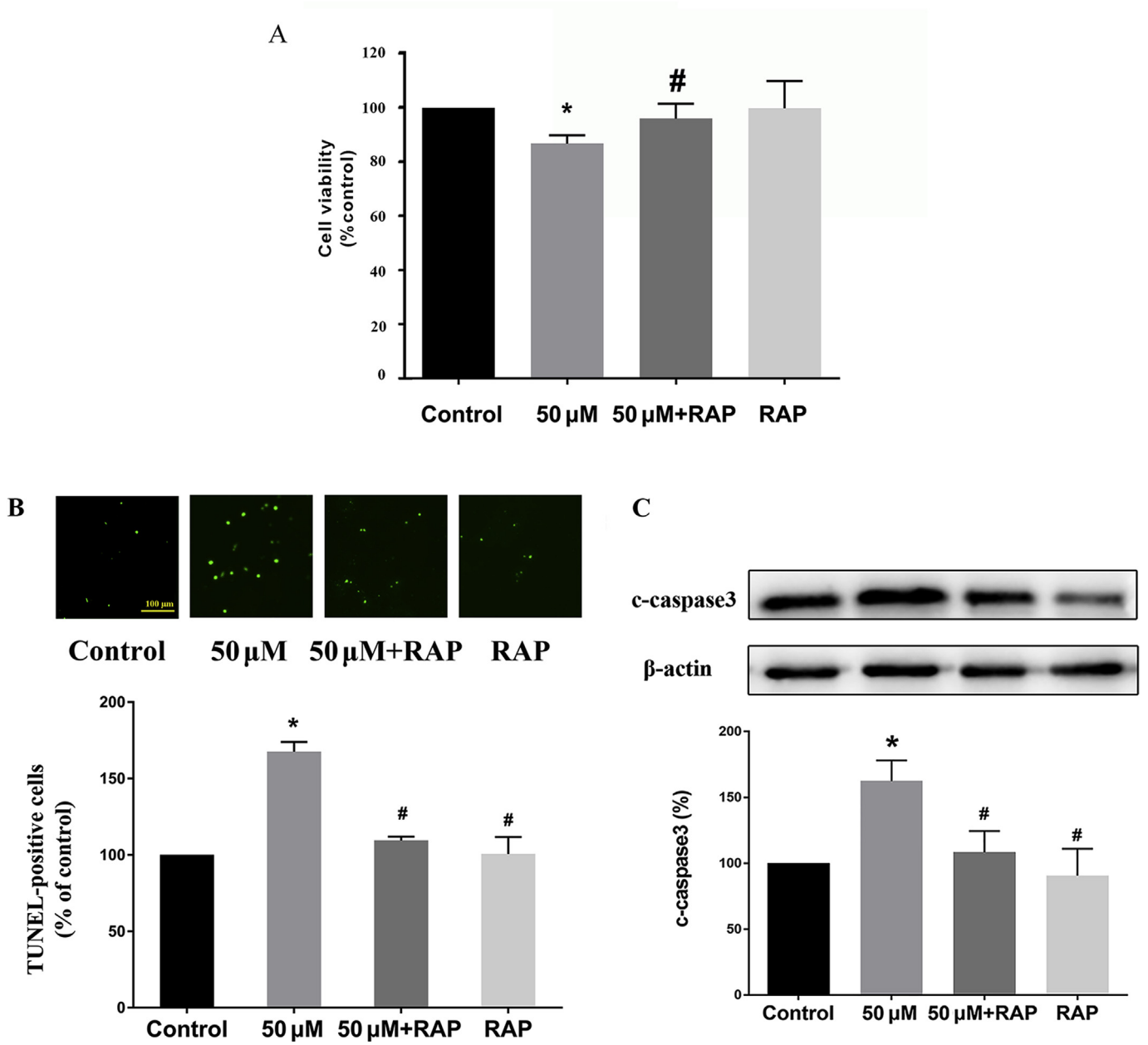

Fig. 7. Activation of autophagy reduced NP-induced apoptosis in cortical neurons. Cultured cortical neurons were treated with 50 μM NP and with/without 300 nM RAP for 24 h (A) MTS assay was used to assess neuronal cell viability in all treatment groups. The values are expressed as mean ± SD (n = 4). (B) Representative images of TUNEL-positive neurons from all treatment groups. Green fluorescence indicates the apoptotic cells. Quantitative analysis of TUNEL-positive cells is shown in the lower bar graphs. (C) Western blotting for the expression of apoptotic marker c-caspase3 in neurons. The upper bands depict representative findings for neurons from all treatment groups. The lower bar graphs show the results of the semi-quantitative measurement of the protein. Each bar represents the mean ± SD (n = 4). *p < 0.05 vs. control group; #p < 0.05. vs. 50 μM group.

Furthermore, to our expectation, cleaved caspase-3, another hallmark of apoptotic cell death, was significantly increased in NP treatment groups. Both the increase of TUNEL-positive neurons and activation of caspase-3 indicated that NP exposure directly increased the apoptosis of neurons.

To further study the NP-induced apoptosis, we examined two critical intrinsic pathways of apoptosis, ER stress pathway and mitochondrial pathway. First, we measured ER stress-related proteins, which are considered as hallmarks of ER stress. In the present study, the levels of GRP78, CHOP, ATF4, and casepase-12 were significantly increased in NP treatment neurons. These data may support the involvement of ER stress in NP-induced apoptosis of primary neurons. Similar to our observations, previous studies showed that NP induced ER stress in other types of cells, such as epithelial intestinal cells (Lepretti et al., 2015), PC12 cells (Kusunoki et al., 2008), and testicular Sertoli cells (Gong et al., 2009). Then, we also evaluated the involvement of mitochondrial pathway in NP-induced apoptosis in the present study. The pro- and anti-apoptotic members in Bcl-2 family, such as Bcl-2 and Bax, are crucial to regulate mitochondrial pathway of apoptosis. It is believed that the Bcl-2/Bax ratio plays a key role in regulation of mitochondria-mediated apoptosis (Tait and Green, 2010). In the present study, NP treatment at various concentrations significantly decreased Bcl-2/Bax ratio. Reduction in mitochondrial transmembrane potential is considered as an early event in mitochondria-mediated apoptosis (Bossy-Wetzel et al., 1998). In addition, as a caspase activator, Cyto-C is a necessary component of mitochondria-mediated

apoptosis (Liu et al., 1996). Both the reduction in mitochondrial transmembrane potential and the release of Cyto-C from the mitochondria were observed in NP treatment neurons. It may be, therefore, reasonable to consider that mitochondrial pathway was involved in NP-induced apoptosis of neurons. Similarly, mitochondrial pathway-dependent apoptosis induced by NP treatment has been found in pancreatic cells (Li et al., 2017). Many lines of evidence have shown that the mitochondrial pathway is closely associated with ER stress in apoptosis (Malhotra and Kaufman, 2011; Wang et al., 2011). Thus, the coincidence of their activation in the present study may suggest their cooperation in NP-induced apoptosis of cultured neurons.

As an endocellular catabolic mechanism, autophagy is responsible for eliminating damaged organelles and unwanted proteins, which enables it play important roles in maintenance of cellular homeostasis (Mizushima et al., 2010; Tang et al., 2014). However, deregulation of autophagy involves in cell death through degrading essential cellular matrix and excessive self-digestion (Martinet and De Meyer, 2009). Excessive autophagy disrupts neuronal homeostasis and contributes to neurodegenerative and neurological disorders (Frake et al., 2015; Ghavami et al., 2014). Autophagy induction and related neuronal death were observed in the CNS of several pathological states (Li et al., 2014). Thus, we examined whether NP exposure directly induced autophagy primary cortical neurons.

The monitor of autophagy is still not very easy currently (Klionsky et al., 2016), so we examined a series of autophagic markers, which involve in the initiation of autophagosome formation, elongation, maturation and fusion, in NP-exposed primary cortical neurons. The up-regulation of LC3-II conversion is considered as a hallmark of autophagy (Huang and Liu, 2015). In the present study, NP treatment increased the LC3-II conversion in primary cortical neurons. However, it should be noted that the increase in the LC3-II levels may also be due to the decrease in autophagic proteolysis (defects in LC3-II degradation) (Mizushima et al., 2010). Hence, we further studied the expression of SQSTM1/p62 and Beclin-1 in primary cortical neurons. As selective substrate for autophagy, the levels of SQSTM1/p62 is often used to assess autophagy activity; the accumulation of SQSTM1/p62 indicates dysfunction of autophagy (Sarkar et al., 2014). Beclin-1 is required for nucleation of autophagosome membranes (He and Levine, 2010). Its binding to the pre-autophagosomal structure enables it function as a key protein in autophagy initiation and progression (Cui et al., 2016; Mei et al., 2016). Therefore, the expression of Beclin-1 is closely linked to autophagy activity. It is also believed that Beclin-1 mediates the key pathways that regulate autophagy (Shrivastava et al., 2012). Though its complicated roles have been suggested in autophagy, Beclin-1 is considered as a positive regulator of autophagy under most circumstances (Kang et al., 2011). Our results showed that NP treatment increased the expression of Beclin-1 and decreased the levels of SQSTM1/p62 in neurons. Furthermore, in order to assess lysosome function, we investigated the expression of LAMP2. LAMP2 protects the lysosomal membrane from autodigestion and maintains the acidic environment of the lysosome, and is often used as an indicator of lysosome function (Endo et al., 2015). In the present study, we found NP treatment increased the expression of LAMP2 in primary cortical neurons, suggesting the activation of lysosome. Taken together, our results showed that NP treatment directly enhanced autophagic flux in primary cortical neurons, as indicated by increased LC3-II conversion, decreased levels of SQSTM1/p62, as well as increased levels of Beclin-1 and LAMP2.

The mammalian target of rapamycin (mTOR) is thought to play a central role in the regulation of autophagy, although some conditions could induce autophagy via an mTOR-independent pathway. The phosphorylated mTOR is a highly reactive protein that inhibits the initiation of autophagy by deactivating related kinase (Kim et al., 2011). We found that NP treatment reduced the levels of p-mTOR protein, and did not change the levels of total mTOR protein. This result is consistent with above findings, and suggests that NP-induced neuronal autophagy is in mTOR dependent manner. Furthermore, our findings therefore suggest that both mTOR (a negative regulator) and Beclin-1 (a positive regulator) may be involved in the NP-induced autophagy in primary cortical neurons.

In this study, we found NP directly elicited autophagy and apoptosis in neurons concurrently. Of note, autophagy is a two-edged sword for the induction of apoptosis. On one hand, many studies have found that autophagic activity directly or indirectly resulted in apoptotic cell death. On the other hand, under some circumstances the activation of autophagy plays a positive role in cell survival through inhibiting apoptosis (Cooper, 2018). For instance, it has been shown that the enhancement of autophagy protected neurons from apoptosis resulted from oxygen-glucose deprivation (Zhou et al., 2017a). In addition, the inhibition of autophagy deteriorated the hypoxia-induced apoptosis in neurons (Li et al., 2018). Although autophagy played neuroprotective roles against apoptosis in these studies, and induction of autophagy and apoptosis coincided in our studies, it was still hard to draw a conclusion about the role of autophagy in NP-induced apoptosis. Thus, both the autophagy inhibitor CQ and the autophagy inducer RAP were applied to the NP-exposed neurons. We found that the inhibition of autophagy by CQ enhanced NP-induced apoptosis. Conversely, RAP-induced autophagy remarkably suppressed NP-induced apoptosis in neurons. These findings clearly demonstrated that autophagy served as a protective role in apoptosis caused by NP exposure in neurons.

5. Conclusions

To conclude, our study demonstrated that NP exposure affected cell viability and induced apoptosis with a concomitant increase of autophagic flux in primary cortical neurons, which may indicate the direct effects of this potential neurotoxin on the CNS. Both ER stress and mitochondrial pathways may contribute to NP-induced apoptosis in neurons. Furthermore, by administrating of pharmacological (CQ and RAP) approaches to modulate autophagy activation, we illuminated the protective role of autophagy in apoptosis of neurons induced by NP. Our findings may provide new evidence to support the idea that specific modulation of autophagy is a neuroprotective strategy to ameliorate NP-induced neurotoxicity.

Declarations of interest

None.

Acknowledgments

This work was supported by Natural Science Foundation of Liaoning Province, China (Grant Number: 201602865) and the Program for Liaoning Innovative Research Team in University (Grant Number: LT2015028).

Appendix A. Supplementary data

Supplementary data to this article can be found online at https://doi.org/10.1016/j.neuint.2018.11.009.

References

Arukwe, A., et al., 2000. In vivo and in vitro metabolism and organ distribution of nonylphenol in Atlantic salmon (Salmo salar). Aquat. Toxicol. 49, 289–304.
Bossy-Wetzel, E., et al., 1998. Mitochondrial cytochrome c release in apoptosis occurs upstream of DEVD-specific caspase activation and independently of mitochondrial transmembrane depolarization. EMBO J. 17, 37–49.
Cao, G., et al., 2001. Intracellular Bax translocation after transient cerebral ischemia: implications for a role of the mitochondrial apoptotic signaling pathway in ischemic neuronal death. J. Cerebr. Blood Flow Metabol. 21, 321–333.
Careghini, A., et al., 2015. Bisphenol A, nonylphenols, benzophenones, and benzotriazoles in soils, groundwater, surface water, sediments, and food: a review. Environ. Sci. Pollut. Res. Int. 22, 5711–5741.
Chang, C.H., et al., 2014. The association between nonylphenols and sexual hormones

levels among pregnant women: a cohort study in Taiwan. PloS One 9, e104245.
Cooper, K.F., 2018. Till death do us part: the marriage of autophagy and apoptosis. Oxid Med Cell Longev 2018, 4701275.
Cui, J., et al., 2016. The BECN1-USP19 axis plays a role in the crosstalk between autophagy and antiviral immune responses. Autophagy 12, 1210–1211.
Endo, Y., et al., 2015. Danon disease: a phenotypic expression of LAMP-2 deficiency. Acta Neuropathol. 129, 391–398.
Frake, R.A., et al., 2015. Autophagy and neurodegeneration. J. Clin. Invest. 125, 65–74.
Ghavami, S., et al., 2014. Autophagy and apoptosis dysfunction in neurodegenerative disorders. Prog. Neurobiol. 112, 24–49.
Gong, Y., et al., 2009. Nonylphenol induces apoptosis in rat testicular Sertoli cells via endoplasmic reticulum stress. Toxicol. Lett. 186, 84–95.
Green, D.R., Reed, J.C., 1998. Mitochondria and apoptosis. Science 281, 1309–1312.
He, C., Levine, B., 2010. The Beclin 1 interactome. Curr. Opin. Cell Biol. 22, 140–149.
Huang, R., Liu, W., 2015. Identifying an essential role of nuclear LC3 for autophagy. Autophagy 11, 852–853.
Huang, Y.F., et al., 2014. Nonylphenol in pregnant women and their matching fetuses: placental transfer and potential risks of infants. Environ. Res. 134, 143–148.
Jie, X., et al., 2010. Toxic effect of gestational exposure to nonylphenol on F1 male rats. Birth Defects Res B Dev Reprod Toxicol 89, 418–428.
Kang, R., et al., 2011. The Beclin 1 network regulates autophagy and apoptosis. Cell Death Differ. 18, 571–580.
Kazemi, S., et al., 2018. The correlation between nonylphenol concentration in brain regions and resulting behavioral impairments. Brain Res. Bull. 139, 190–196.
Kesidou, E., et al., 2013. Autophagy and neurodegenerative disorders. Neural Regen Res 8, 2275–2283.
Kim, J., et al., 2011. AMPK and mTOR regulate autophagy through direct phosphorylation of Ulk1. Nat. Cell Biol. 13, 132–141.
Klionsky, D.J., et al., 2016. Guidelines for the use and interpretation of assays for monitoring autophagy (3rd edition). Autophagy 12, 1–222.
Kudo, C., et al., 2004. Nonylphenol induces the death of neural stem cells due to activation of the caspase cascade and regulation of the cell cycle. J. Neurochem. 88, 1416–1423.
Kusunoki, T., et al., 2008. p-Nonylphenol induces endoplasmic reticulum stress-mediated apoptosis in neuronally differentiated PC12 cells. Neurosci. Lett. 431, 256–261.
Lepretti, M., et al., 2015. 4-Nonylphenol reduces cell viability and induces apoptosis and ER-stress in a human epithelial intestinal cell line. Toxicol. Vitro 29, 1436–1444.
Li, I.H., et al., 2014. Autophagy activation is involved in 3,4-methylenedioxymethamphetamine ('ecstasy')–induced neurotoxicity in cultured cortical neurons. PloS One 9, e116565.
Li, P., et al., 2018. Chloroquine inhibits autophagy and deteriorates the mitochondrial dysfunction and apoptosis in hypoxic rat neurons. Life Sci. 202, 70–77.
Li, X., et al., 2017. Nonylphenol induces pancreatic damage in rats through mitochondrial dysfunction and oxidative stress. Toxicol Res (Camb) 6, 353–360.
Litwa, E., et al., 2014. Apoptotic and neurotoxic actions of 4-para-nonylphenol are accompanied by activation of retinoid X receptor and impairment of classical estrogen receptor signaling. J. Steroid Biochem. Mol. Biol. 144, 334–347.
Litwa, E., et al., 2016. RXRalpha, PXR and CAR xenobiotic receptors mediate the apoptotic and neurotoxic actions of nonylphenol in mouse hippocampal cells. J. Steroid Biochem. Mol. Biol. 156, 43–52.
Liu, X., et al., 1996. Induction of apoptotic program in cell-free extracts: requirement for dATP and cytochrome c. Cell 86, 147–157.
Malhotra, J.D., Kaufman, R.J., 2011. ER stress and its functional link to mitochondria: role in cell survival and death. Cold Spring Harb Perspect Biol 3, a004424.
Mao, Z., et al., 2010. Behavioral impairment and oxidative damage induced by chronic application of nonylphenol. Int. J. Mol. Sci. 12, 114–127.
Mao, Z., et al., 2008. Chronic application of nonylphenol-induced apoptosis via suppression of bcl-2 transcription and up-regulation of active caspase-3 in mouse brain. Neurosci. Lett. 439, 147–152.
Martinet, W., De Meyer, G.R., 2009. Autophagy in atherosclerosis: a cell survival and death phenomenon with therapeutic potential. Circ. Res. 104, 304–317.
Mei, Y., et al., 2016. Conformational flexibility of BECN1: essential to its key role in autophagy and beyond. Protein Sci. 25, 1767–1785.
Mizushima, N., Komatsu, M., 2011. Autophagy: renovation of cells and tissues. Cell 147, 728–741.
Mizushima, N., et al., 2010. Methods in mammalian autophagy research. Cell 140, 313–326.
Nakagawa, T., et al., 2000. Caspase-12 mediates endoplasmic-reticulum-specific apoptosis and cytotoxicity by amyloid-beta. Nature 403, 98–103.
Nutt, L.K., et al., 2002. Bax and Bak promote apoptosis by modulating endoplasmic reticular and mitochondrial Ca2+ stores. J. Biol. Chem. 277, 9219–9225.
Peng, F., et al., 2016. A study on phthalate metabolites, bisphenol A and nonylphenol in the urine of Chinese women with unexplained recurrent spontaneous abortion. Environ. Res. 150, 622–628.
Perry, S.W., et al., 2011. Mitochondrial membrane potential probes and the proton gradient: a practical usage guide. Biotechniques 50, 98–115.
Ryter, S.W., et al., 2014. The impact of autophagy on cell death modalities. Int J Cell Biol 502676 2014.
Sarkar, C., et al., 2014. Impaired autophagy flux is associated with neuronal cell death after traumatic brain injury. Autophagy 10, 2208–2222.
Shen, H., et al., 2000. Dual role of glutathione in selenite-induced oxidative stress and apoptosis in human hepatoma cells. Free Radic. Biol. Med. 28, 1115–1124.
Shrivastava, S., et al., 2012. Hepatitis C virus upregulates Beclin1 for induction of autophagy and activates mTOR signaling. J. Virol. 86, 8705–8712.
Singh, A.K., et al., 2017. Autophagy activation alleviates amyloid-beta-induced oxidative stress, apoptosis and neurotoxicity in human neuroblastoma SH-SY5Y cells. Neurotox. Res. 32, 351–361.
Sise, S., Uguz, C., 2017. Nonylphenol in human breast milk in relation to sociodemographic variables, diet, obstetrics histories and lifestyle habits in a Turkish population. Iran. J. Public Health 46, 491–499.
Song, S., et al., 2017. Crosstalk of autophagy and apoptosis: involvement of the dual role of autophagy under ER stress. J. Cell. Physiol. 232, 2977–2984.
Tabas, I., Ron, D., 2011. Integrating the mechanisms of apoptosis induced by endoplasmic reticulum stress. Nat. Cell Biol. 13, 184–190.
Tabassum, H., et al., 2017. Role of melatonin in mitigating nonylphenol-induced toxicity in frontal cortex and hippocampus of rat brain. Neurochem. Int. 104, 11–26.
Tait, S.W., Green, D.R., 2010. Mitochondria and cell death: outer membrane permeabilization and beyond. Nat. Rev. Mol. Cell Biol. 11, 621–632.
Tang, L., et al., 2017. Regulation of nonylphenol-induced reproductive toxicity in mouse spermatogonia cells by miR-361-3p. Mol. Reprod. Dev. 84, 1257–1270.
Tang, P., et al., 2014. Autophagy reduces neuronal damage and promotes locomotor recovery via inhibition of apoptosis after spinal cord injury in rats. Mol. Neurobiol. 49, 276–287.
Wang, H., et al., 2011. Role of death receptor, mitochondrial and endoplasmic reticulum pathways in different stages of degenerative human lumbar disc. Apoptosis 16, 990–1003.
Xi, X., et al., 2013. The interplays between autophagy and apoptosis induced by enterovirus 71. PloS One 8, e56966.
Yang, Z., Klionsky, D.J., 2010. Eaten alive: a history of macroautophagy. Nat. Cell Biol. 12, 814–822.
Yoon, Y.H., et al., 2010. Induction of lysosomal dilatation, arrested autophagy, and cell death by chloroquine in cultured ARPE-19 cells. Invest. Ophthalmol. Vis. Sci. 51, 6030–6037.
Yu, Y., et al., 2017. The alteration of autophagy and apoptosis in the hippocampus of rats with natural aging-dependent cognitive deficits. Behav. Brain Res. 334, 155–162.
Zhang, Y., et al., 2017. Bisphenol A affects cell viability involved in autophagy and apoptosis in goat testis sertoli cell. Environ. Toxicol. Pharmacol. 55, 137–147.
Zhou, C., et al., 2018. CYP2J2-derived EETs attenuated ethanol-induced myocardial dysfunction through inducing autophagy and reducing apoptosis. Free Radic. Biol. Med. 117, 168–179.
Zhou, T., et al., 2017a. Effect of autophagy regulator on the injury of rat hippocampal neurons induced by oxygen-glucose deprivation. Zhonghua Wei Zhong Bing Ji Jiu Yi Xue 29, 738–743.
Zhou, X., et al., 2017b. Autophagy plays a positive role in zinc-induced apoptosis in intestinal porcine epithelial cells. Toxicol. Vitro 44, 392–402.